Journal of Materials Chemistry B

Accepted Manuscript

ROYAL SOCIETY OF CHEMISTRY

www.rsc.org/materialsB

PEG-poly (amino acid)s-encapsulated Tanshinone IIA as potential therapeutics for the treatment of hepatoma

Yan Wang,[1,2,a] Frankie Costanza,[3,a] Haifan Wu,[3] Daqian Song[1], Jianfeng Cai[3,*] and Qi Li [1,*]

[1]Department of Medical Oncology, Shuguang Hospital, Shanghai University of Traditional Chinese Medicine, 528 Zhangheng Road，Shanghai, 201203, China

[2]Tumor Institute of Traditional Chinese Medicine, Longhua Hospital Shanghai University of Traditional Chinese Medicine, Shanghai 200032 , China

[3]Department of Chemistry, University of South Florida, 4202 E. Fowler Ave, Tampa, FL 33620

[a] These authors contributed equally to the work.

lzwf@hotmail.com and jianfengcai@usf.edu

ABSTRACT

Tanshinone IIA is a potent anti-tumor agent; however, its therapeutic applications have been hindered by its intrinsic poor solubility and short half life. Herein we report the design and synthesis of amphiphilic PEG-poly (amino acid)s (PPAAs), which was used as a nanocarrier to encapsulate Tanshinone IIA. PPAAs-encapsulated Tanshinone IIA formed defined nanoparticles and effectively arrested the growth of the hepatoma tumor in MHCC97-H hepatoma-bearing mice, which has therefore significantly increased their survival time. Moreover, these Tanshinone-loaded nanoparticles are also capable of suppressing hepatic tumor cell migration and metastasis. In all cases, they significantly improve efficacy compared to Tanshinone alone. Our results show that Tanshinone IIA encapsulated by PPAAs is a potential novel nanomedicine for the treatment of hepatoma. Furthermore, this use is only a proof of concept, and PPAAs can be used as a potential drug delivery system for a much broader array of hydrophobic drugs.

INTRODUCTION

Tanshinone IIA (Figure 1) is a lipo-soluble small molecule isolated from *salvia miltiorrhiza*, and displays broad-spectrum anti-tumor activity.[1-6] It is believed to have multiple intra- and extra- cellular targets[7] and therefore is less probable to develop drug-resistance in tumor cells. However, Tanshinone IIA (TSIIA) has

some intrinsic drawbacks such as poor water solubility and a short half-life. [8] This has prompted the ongoing research to develop new delivery systems to increase the solubility of TSIIA and to improve its anti-tumor efficacy. [6-8] In order to advance the application and efficacy of TSIIA as a novel anti-cancer therapeutic, the exploration of new polymer delivery systems are needed. As such, herein we report the design and synthesis of amphiphilic PPAAs PEG-poly(amino acid)s, which were used as a novel nanocarrier to encapsulate and deliver TSIIA.

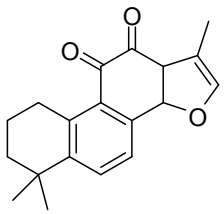

Figure 1. The structure of Tanshinone IIA.

Compared to other polymer delivery systems, poly (amino acid)s have many attractive features. The synthesis of poly (amino acid)s is very straightforward, which can be achieved through the ring-opening polymerization of N-carboxyanhydrides (NCAs).[9] NCAs are commercially available, or they can be obtained in one step upon treatment of natural amino acids with phosgene or triphosgene. They can also be added batch by batch, which therefore allows for easy synthesis of poly (amino acid)s with multiple blocks. As there are 20 natural amino acids, the potential is limitless to obtain poly (amino acid)s that contain a diverse array of functional groups with tunable charges.. Additionally, they are biocompatible and completely biodegradable, and have low toxicities, which further augment their application for drug delivery. [10-12] Furthermore, poly (amino acid)s can be easily modified with other functional groups. For example, PEG can be attached to the terminus of poly (amino acid)s, which helps to prevent self-aggregation and prolongs its half-life, etc.[13] Therefore, we expect that PEG-poly(amino acid)s will be an excellent carrier for the delivery of TSIIA and will improve its anti-tumor efficacy.

EXPERIMENTAL SECTION

Materials

Amino acids were purchased from Purebulk and Chemimpex. Other chemicals were purchased either from Fisher Scientific or Sigma-Aldrich, and used directly without further purification. Tanshinone ⅡA (98.4%) was purchased from Xian Guanyu Pharmaceutical Co,. Ltd, China. MHCC97-H hepatoma cells, and BALB/c male athymic nude mice from Shanghai Cancer Institute; and CCK-8 Cell Proliferation Assay Kit was purchased from Cayman Chemical. D-Luciferin Potassium salt was purchased from Synchem-Pharma Co., Ltd.

Animals

BALB/c male athymic nude mice (5 weeks old, body weight 14.8 ± 0.9 g) were purchased from the Department of Experimental Animals of Shanghai Fudan University. All animals were housed at 22°C on a 12-h light/dark cycle. All experiments were performed according to the recommendations of the local animal protection legislation for conducting animal studies approved by the Ethics Committee of Shanghai University of Traditional Chinese Medicine (SYXK 2005-0008).

Experimental

Synthesis of poly (amino acid)s

CH3O-PEG5000-NH_2 (0.4g, 0.00008 mol) was dissolved in 10 ml of anhydrous dioxane and purged with N_2. Separately 20 equiv. (0.42g, 0.0016 mol) of Glu (OBz)-NCA was dissolved in 5 ml anhydrous dioxane, passed through a 2 μM filter to remove any decomposed NCA, thoroughly purged with N_2 and then added via syringe. The reaction was then allowed to proceed for 3 days under an active N_2 atmosphere. Then 10 equiv. (0.21g, 0.0008 mol) of Glu (OBz)-NCA and 15 equiv. of Phe-NCA (0.229g, 0.0012 mol) were dissolved in 5 ml anhydrous dioxane, passed through a 2 μM filter, purged, and added via syringe. Polymerization was allowed to continue for another 3 days. The clear solution was then precipitated into ether and the product was collected via filtration.

Removal of benzyl ester groups:

The polymer was dissolved in 10 ml of TFA and to this solution, 10 equiv. of HBr in AcOH (33% v/v

conc.) was added and stirred for 4 hours. The product was then precipitated into ether and collected via filtration.[11,12]

Dialysis:

The polymer was dissolved in minimal DMSO and added to dialysis tubing (MWCO = 3,500) followed by immersion in water. Dialysis was carried out for 3 days, replacing the water daily. Any precipitate was then filtered out, and the clear filtrates were lyophilized to afford the final products.

Preparation of PEG-poly (amino acid)s-encapsulated TSIIA nanoparticles

5 mg TSIIA and 45 mg PEG-poly (amino acid)s were dissolved in 700 μL DMSO, followed by drop-wise addition of 30 mL 30% tert-butanol/water. The resulting solution was stirred for 3h at room temperature, and then lyophilized to produce a solid puffy cake. The solid was re-dissolved in 30% tert-butanol/water, stirred for 3h and lyophilized. The resulting solid was again dissolved in pure water, stirred for 3h, and the lyophilization provided the desired TSIIA-loading poly (amino acid)s nanoparticles.

Cytotoxicity

The cytotoxicity of nanoparticles against MHCC97-H hepatoma cells was determined using CCK-8 cell viability assay[19]. Briefly, MHCC97-H hepatoma cells (1×10^4/well) were seeded in 96 well and incubated overnight. The cells were then incubated for 24 h and 48h at 37°C/5% CO_2 using different concentrations (5, 10, 20μg/mL)of TSIIA, (50, 100, 200μg/mL)PEG-poly(amino acid)s nanoparticles, and (50, 100, 200μg/mL; containing 5, 10, 20μg/mL TSIIA)PEG-poly (amino acid)s-encapsulated TSIIA nanoparticles. 10 μl cell counting kit-8 (CCK-8; Dojindo Molecular Techinologies, Inc, Japan) was added to each well and the plates were incubated for an additional 1h at 37°C/5%. Finally, the cell viability was measured as the absorbance at 450 nm (A450) using a microplate reader (Bio-Rad, Model 680, Hercules, CA, USA). All experiments were performed in triplicate.

Tumor model

The following study consisted of tissue distribution, targeted imaging and therapeutic evaluation was carried out when the tumor grew to approximately 0.1 cm^3. Four to six week old Male BALB/c nude mice were subcutaneously injected with $2x10^6$ human liver cancer cells MHCC97-H. After 7 -10 days when implanted tumors reached 1-1.2 cm in diameter, the mice were sacrificed under sterilized condition, the

xenografic tumors were dissected out, minced into 1mm^3 pieces, and were then implanted into the right flanks of nude mice. When these tumors reached 1 cm in diameter, they were minced to 1-mm^3 chunks to establish the model of the orthotopic liver cancer. The procedure was first done by making a 1-cm incision along the lower edge of the left ribcage, which exposes the left lobe of liver. Then, a space was generated between the liver and its capsule using forceps, into which tumor chunks were inserted. Hemostatic measures were applied during surgery and no active bleeding was detected before closure.

Biodistribution

To evaluate TSIIA biodistribution, the six HCC-bearing mice (three mice per group) were injected with TSIIA and TSIIA NPs at doses equivalent to 1 mg TSIIA per kg in 0.2 ml of PBS via the caudal vein. The heart, liver, spleen, lung, kidney, colon, and tumors were collected 24 h post-injection. Biodistribution was calculated as the percentage of injected dose per gram of tissue (%ID/g) by Liquid Chromatography Tandem Mass Spectrometry (LC-MS-MS). Values are expressed as mean ± SD (n = 3).

***In vivo* study of the therapeutic efficacy in mice**

The fourty-eight mice were classified into 4 groups on the basis of the solutions they were administered: control group (normal saline, 13.5 mL/kg), blank nanoparticles group (blank NPs, 10mg/kg), TSIIA solution group (TSIIA, 1 mg/kg), and PEG-poly (amino acid)s-encapsulated TSIIA nanoparticles group (TSIIA NPs, 10mg/kg, containing TSIIA 1mg/kg), by injection through the vena caudalis at 1vic/2day. fourteen days after the injection, six mice in each group were randomly evaluated for survival time. Life extended rate (L) was calculated as follows:

$$L=(STtest-STcontrol)/STcontrol\times 100\%$$

where *STcontrol* and *STtest* are the average survival time (days) for the mice administered with normal saline and with tested agents respectively. The toxicities of the NPs were evaluated by monitoring changes in body weight.

The remaining six mice in each group were killed, and the tumors were removed for examination. The longest (a) and the longest (b) vertical dimensions of the tumor were measured. The size (V) of the tumor was calculated using the following equation:

$$V = ab^2/2$$

Representative formalin-fixed, paraffin-embedded tissue blocks from each tumor were analyzed by conventional hematoxylin-erosin (HE) staining. The degree of necrosis in each tumor was visually graded as follows: +, no necrosis present or slight necrosis in fragments; ++, mid-range necrosis, absence of nuclei from many cells with or without massive cytoplasmic damage; and +++, severe necrosis, total loss of cytoplasm of the cancer cells.

***In vivo* optical imaging**

The *in vivo* optical imaging in MHCC97-H hepatoma-bearing mice was evaluated using CRI Maestro TM In vivo Fluorescence Imaging System from Cambridge Research & Instrumentation (Massachusetts, USA). The twenty-four mice were classified into 4 groups: control group (normal saline, 13.5 mL/kg), blank nanoparticles group (blank NPs, 10mg/kg), TSIIA solution group (TSIIA, 1 mg/kg), and PEG-poly (amino acid)s-encapsulated TSIIA nanoparticles group (TSIIA NPs, 10mg/kg, containing TSIIA 1mg/kg), by injection through the vena caudalis at 1vic/2day. Prior to in vivo imaging, the mice were anesthetized with phenobarbital sodium. D-luciferin solution (150 mg/kg) was injected i.p 5 min. before imaging. Exposure times of the bioluminescence imaging ranged from 10 to 30s. Fluorescence images were obtained at an excitation wavelength of 490 nm and emission wavelength of 535 nm. Exposure times ranged from 1 to 2 min. and the fluorescence images were captured using CRI Maestro TM In vivo Fluorescence Imaging System *in vivo* optical imaging.

RESULTS AND DISCUSSION

Synthesis of PEG-poly (amino acid)s and encapsulation of Tanshinone IIA

To test our hypothesis, we synthesized a PPAA containing both hydrophilic and hydrophobic groups (Figure 2) via ring-opening polymerization of N-carboxyanhydrides (NCAs). [11] In an aqueous solution, the PEG-poly (amino acid)s are expected to form amphiphilic micelles containing a hydrophobic core and a hydrophilic corona. In our attempt, we prepared PPAAs containing glutamate and phenylalanine residues. In brief, Glu(OBz)-NCA and Phe-NCA were synthesized by reacting amino acids phenylalanine or H-Glu(OBz)-OH with triphosgene (Figure 2a). [11] Then, CH_3O-PEG5000-NH_2 was used to initiate the ring-opening polymerization of the NCAs (Figure 2b) to produce the desired poly (amino acid)s. The core-shell nanostructures were achieved by first adding 20 equiv. Glu(OBz)-NCA and allowing the reaction to proceed for three days at room temperature. Subsequently, 10 equiv. Glu(OBz)-NCA and 15 equiv. Phe-NCA were added simultaneously in order to form an anionic-hydrophobic hybrid core in solution. This hybrid core design is different from other previously reported PEG-poly(amino acid)s di-block copolymers, in which the core contains only exclusively hydrophobic groups such as Phe. [11] We anticipated the hybrid core to be advantageous as it is hydrophobic enough to encapsulate TSIIA, yet hydrophilic enough (due to the presence of anionic charges) to aid in its water solubility. This type of core can minimize the probability of aggregation, enhance the targeted delivery of TSIIA, and aid in its release as it is more weakly bounded to the core compared to previously reported literature (citation would be needed).The sequence of the poly (amino acid)s (PDI: 1.05 by GPC) was also confirmed by NMR (Figure 2c).

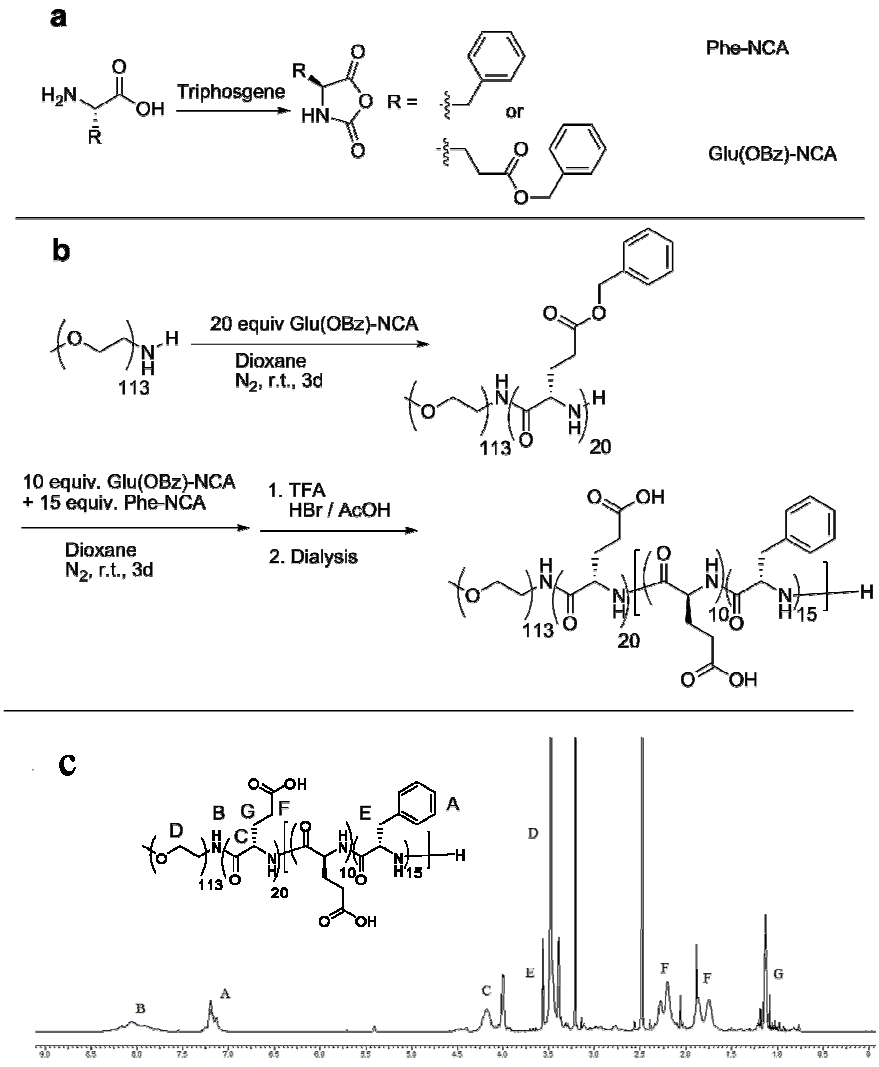

Figure 2. a, synthesis of Phe-NCA and H-Glu(OBz)-NCA; **b,** synthesis of the PEG-poly (amino acid)s. **c,** ^{1}H-NMR (800 MHz, DMSO-d_6) of the PEG-poly (amino acid)s. Amino acid residues shown in the bracket were added in one batch.

The PPAAs were then used to encapsulate TSIIA by adopting a previously reported protocol. [14, 15] Briefly, TSIIA and PEG-poly (amino acid)s were dissolved in DMSO, followed by drop-wise addition of 30% tert-butanol/water. The solution was lyophilized to produce TSIIA-loading nanoparticles.

The nanomorphology of these NPs was confirmed by SEM. As expected, irrelevant of encapsulation of TSIIA, poly (amino acid)s all form nanoparticles in water with sizes ranging from 50 to 100 nm (Figure 3). Interestingly, poly (amino acid)s containing TSIIA show a smaller size distribution, probably due to the

strong hydrophobic interactions between TSIIA and Phe residues in the polymer, which leads to a tighter core in the nanoparticles.

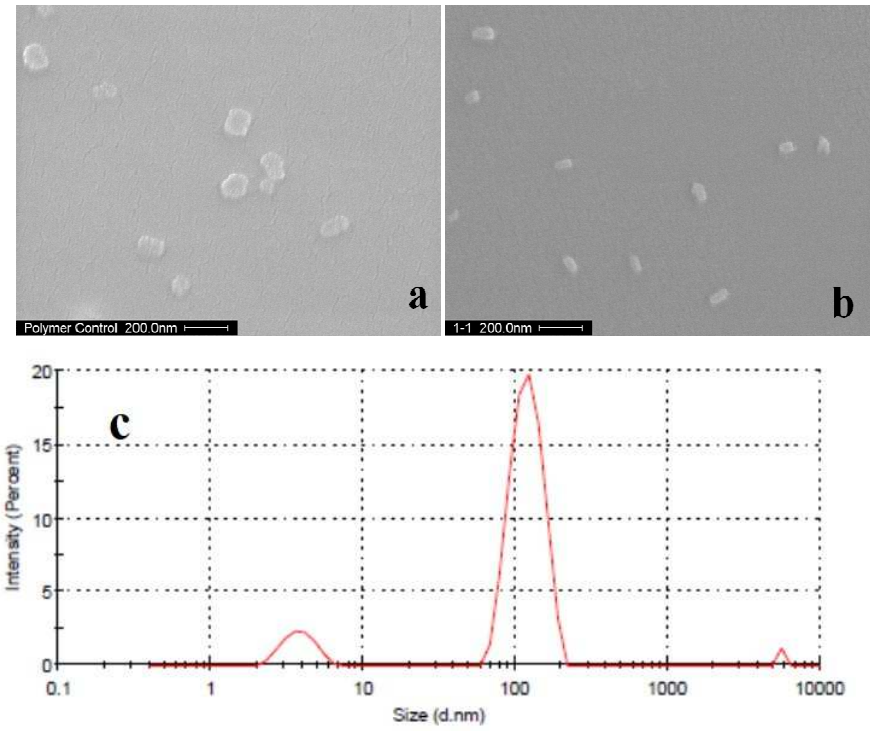

Figure 3. Nanomorphology of poly (amino acid)s. a, SEM image of poly (amino acid)s; b, SEM image of TSIIA-loading poly (amino acid)s. c, Size distribution of poly (amino acid)s obtained by DLS.

Cytotoxicity

Cytotoxicity results showed that PEG-poly (amino acid)s-encapsulated TSIIA nanoparticles effectively increase the cytotoxicity for MHCC97-H hepatoma cells as compared with TSIIA alone (Figure 4). At 24 h post-incubation, the cell viability of MHCC97-H hepatoma cells was higher than that of 48 h post-incubation. The MHCC97-H hepatoma cells treated with increasing doses of PEG-poly(amino acid)s nanoparticles showed 94% to 98% viability, respectively. This finding suggested that the blank PEG-poly(amino acid)s nanoparticles were non-toxic at each of the tested concentrations. Specifically, the cytotoxicity of PEG-poly (amino acid)s-encapsulated TSIIA nanoparticles was significantly improved over time, revealing that the PEG-poly (amino acid)s-encapsulated TSIIA nanoparticles can enhance the cytotoxicity of TSIIA for MHCC97-H hepatoma cells. The higher cytotoxicity is very beneficial for antitumor therapy *in vivo*.

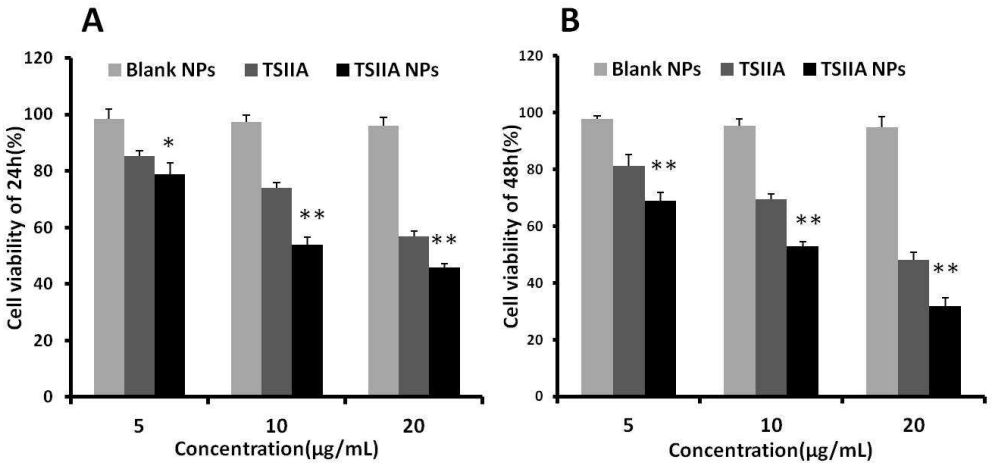

Figure 4. In vitro cytotoxicity of nanoparticles in MHCC97-H hepatoma cells. (A) 24 h-treatment, and (B) 48 h-treatment. *$p<0.05$ when compared with TSIIA; **$p<0.01$ when compared with TSIIA.

Biodistribution

Biodistribution of free TSIIA and PEG-poly (amino acid)s-encapsulated TSIIA nanoparticles in HCC-bearing mice in various tissues and organs is shown in Figure 5. After 24 h of injection, greater concentrations of free TSIIA were found in heart, lung and kidney than TSIIA NPs. In tissues, TSIIA concentration 24h post-TSIIA NPs injection followed the order of tumor > liver > kidney > lung > spleen > colon > heart, whereas tumor accumulation of free TSIIA was markedly lower. For TSIIA NPs, around 16.3%ID/g was found in tumor at 24 h post-injection whereas for free TSIIA found was around 1.2%ID/g. Overall, there were significant differences in the uptake of free TSIIA and TSIIA NPs by different tissues and organs.

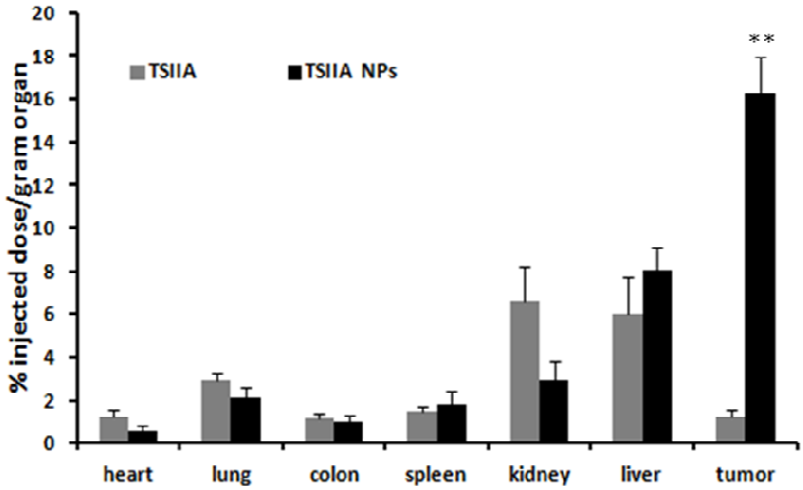

Figure 5. Biodistribution of TanshinoneIIA NPs. Data are shown as the percentage of injected dose per gram of organ weight (%ID/g). $^{**}P < 0.01$ compared to the other groups. Data is presented as mean ± SD (n = 3).

Therapeutic efficacy in hepatoma-bearing mice

To assess the potential of poly (amino acid)s with encapsulated TSIIA as a novel anti-cancer agent, we evaluated its *in vivo* therapeutic efficacy using a hepatoma-bearing mouse model, as TSIIA was previously reported to have significant activity against hepatoma. [6, 16-18] We first examined the ability of encapsulated TSIIA to prevent the growth of hepatic tumor. After administration of the polymer nanoparticles, the tumor volume was measured at predetermined intervals so as to calculate the inhibition rate. As illustrated in Figure 6A, compared to the control group in which only saline was administered, poly (amino acid)s alone (denoted as blank NPs hereafter) did not stop tumor growth. Consistent with previous findings, TSIIA is an effective anti-tumor agent, which suppressed the growth of the hepatic tumor by 40%. However, as seen after 4 weeks of treatment, encapsulated TSIIA (denoted as TSIIA NPs) was a superior therapeutic agent, as it successfully arrested the growth of the hepatic tumor by 75%. Compared to TSIIA alone, the anti-tumor efficacy of TSIIA NPs inhibited another 50% tumor growth. The results demonstrate that the delivery of TSIIA NPs by PPAAs is an effective approach to treat hematoma, suggesting the potential of further development of PPAAs for anti-cancer drug delivery.

With regard to toxic side effects, the body weight of the animals showed no significant difference between the control and treated groups (Figure 6B), but the difference of tumor size is conspicuous, suggesting that the PPAAs effectively enhanced antitumor efficiency with minimal toxicity.

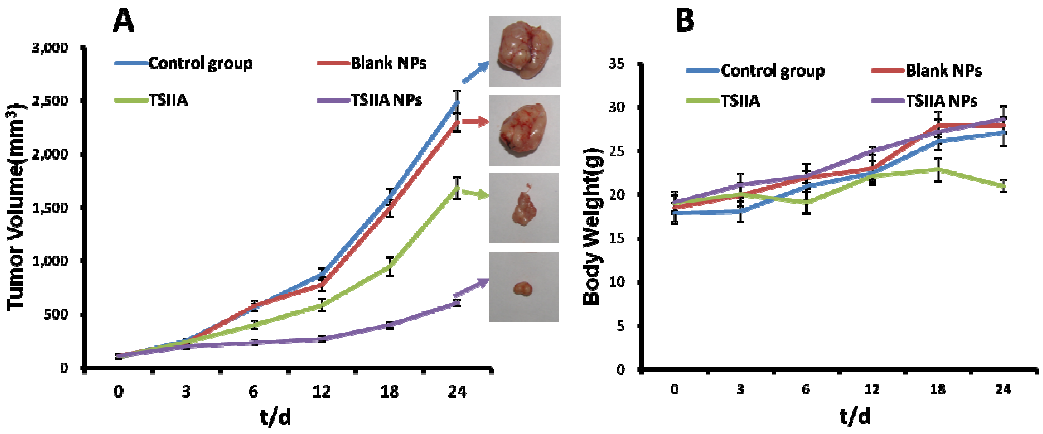

Figure 6 Tumor inhibitory effect of TSIIA nanoparticles in vivo. (A) The tumor growth curves (mm^3), (B) body weights (g). Data is represented as the mean ± standard deviation (n = 6).

The effect on the survival time of mice with hepatoma was also determined. As shown in Figure 7A, all the mice eventually died of hepatoma. Among the four test groups, TSIIA NPs exhibited the most promising results to improve the overall survival rate, with the longest survival time of 37.50±1.87 days (P<0.01), compared with the saline control group that had the shortest survival time of 24.83±2.56 days. Interestingly, TSIIA alone did not improve the survival time, which may be due to the insolubility and the short half-life. Blank NPs as well only showed a very marginal effect on the mouse survival. The results indicate that among the four groups, TSIIA NPs show the most potent anticancer activity, which further augments its potential as an anti-cancer nanomedicine (Figure 7B). Meanwhile, the results further support that PPAAs are excellent nanocarriers for therapeutic development.

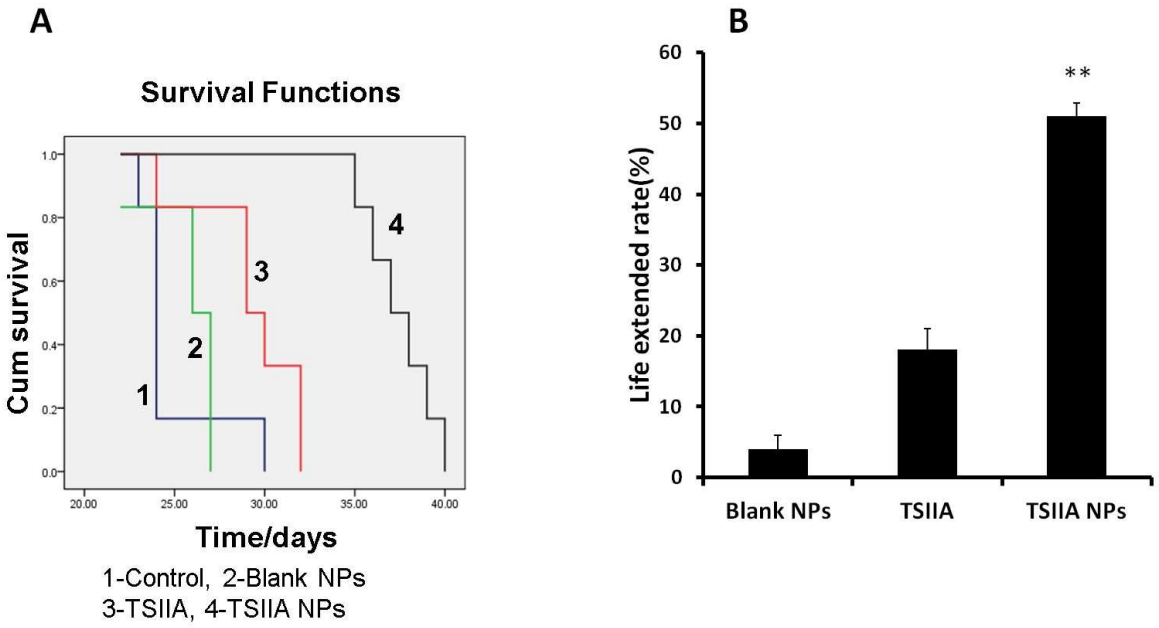

Figure 7. (A) Kaplan-Meier overall survival analysis and (B) Life extended rate of the MHCC97-H hepatoma-bearing mice treated with TSIIA nanoparticles. $^{**}p < 0.01$vs the other groups. Data is represented as the mean ± standard deviation (n = 6)

In addition, the degree of tumor putrescence in each group was also examined by electron microscope with conventional HE staining as illustrated in Figure 8. The necrosis area in the TSIIA NPs group was significantly greater than that of the other groups, which further demonstrated the powerful capability of preventing the growth of the tumor. The TanshinoneIIA group also displayed a certain extent of necrosis , which might due to its high concentration in solution and its intrinsic anti-tumor efficacy.

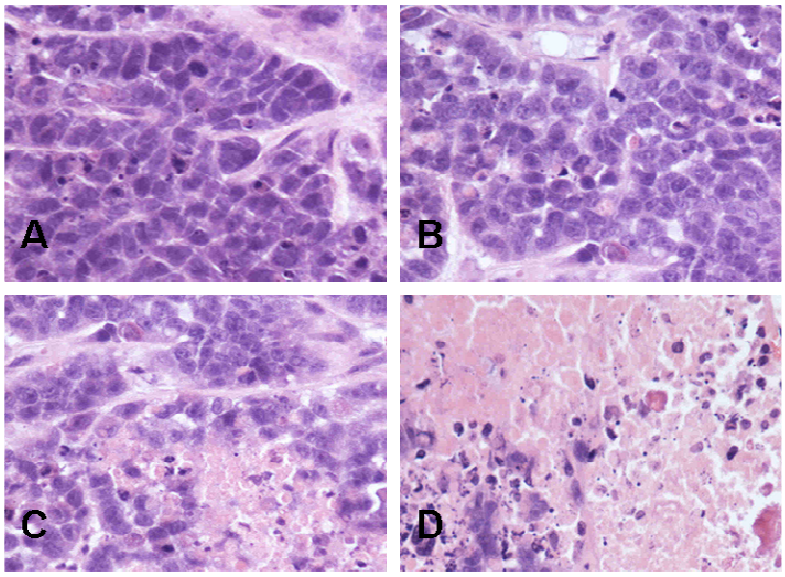

Figure 8. Representative histopathological sections of the tumors from tumor-bearing mice (HE Stained, magnification×200). (A) minimal necrosis after treatment with normal saline; (B) minimal necrosis after treatment with blank nanoparticles;(C) mid-range necrosis after treatment with free Tanshinone IIA; (D) severe necrosis after treatment with TSIIA nanoparticles.

In vivo optical imaging

Subcutaneous xenografting has been a widely used model to evaluate the tumor growth *in vivo*. In our current report, we established an orthotopic murine liver cancer model by directly implanting human hepatic cancer cell line MHCC97-H-Luc into the mouse liver. This model has shown the ability to not only retain the morphology and biological characteristics of primary human liver cancer, but also to mimic its microenvironment with the cancer cells capable of metastasizing.[19] To continuously observe and record *in vivo* tumor growth, we used a luciferase labeled human hepatic cancer cell line MHCC97-H-Luc for this model. Twenty days after implantation, when orthotopic tumors grew to an average size of 1 mm^3, tumor-bearing animals were randomly allocated into 4 different treatment/injection groups: saline control, blank NPs, TSIIA, TSIIA NPs. Tumor size was determined on day 3, 6, 18, 24 and post-treatment. As shown in Figure9, on day 3, no significant difference of tumor size was observed among any experimental

group. On day 14, we found significantly smaller tumors in the mice treated with TSIIA NPs compared to the controls ($P<0.01$). On day 24, tumors in the control groups grew to considerable size and had detectable metastasis, while tumors in TSIIA treatment group were smaller in spite of having some metastasis. In contrast, tumors were much smaller in the TSIIA-nanoparticle group ($P<0.01$), and more interestingly, exhibited the smallest metastatic sites. The results suggest that TSIIA NPs also inhibit tumor metastasis, as well as growth.

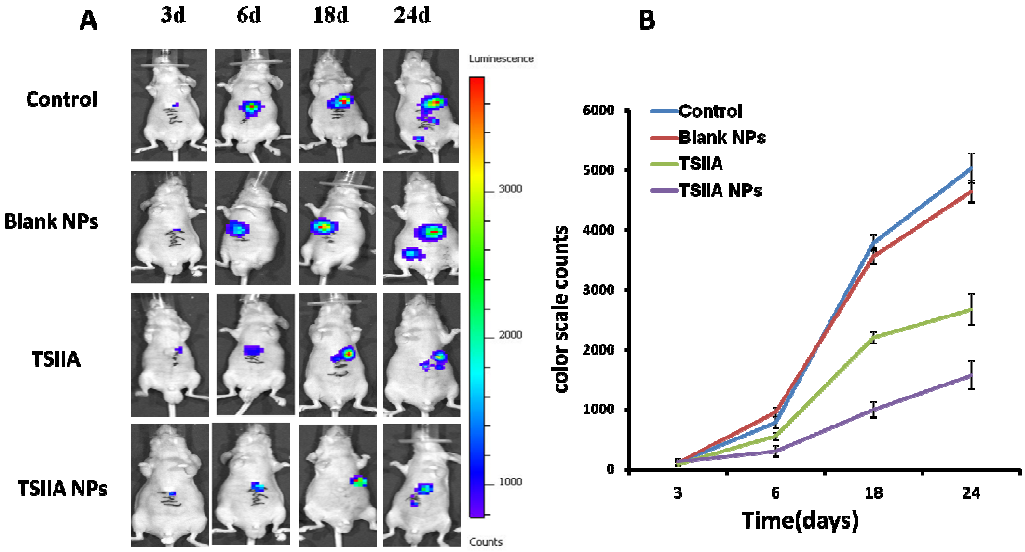

Figure 9. Image of hepatoma-bearing mice. The color bars (from blue to red) represent the change of fluorescence intensity from low to high. Data is represented as the mean ± standard deviation (n = 6)

CONCLUSION

In conclusion, we report the design and synthesis of PEG-poly (amino acid)s copolymer nanoparticles. The nanoparticles encapsulated Tanshinone IIA and enhanced its antitumor activity *in vivo* using a hepatoma-bearing mouse model. The increase in anti-tumor efficacy is not due to the polymer nanoparticles themselves; instead, it comes from Tanshinone IIA after encapsulated delivery. Our results suggest that PEG-poly (amino acid)s encapsulated Tanshinone IIA are a potential novel nanomedicine for the treatment of hepatoma, and meanwhile, PEG-poly (amino acid)s are an excellent class of nanocarriers

for further development and delivery of hydrophobic anti-cancer therapeutics.

AUTHOR INFORMATION

Corresponding Author

*E-mail: jianfengcai@usf.edu and lzwf@hotmail.com

ACKNOWLEDGMENTS

The work was supported by National Natural Science Foundation of China (Project 81001594) (YW) and the USF start-up fund (JC). This research work was also supported by The Science Foundation for Shanghai Committee of Science Project (12140902500, 114119A9500, 11nm0504500), Program of Shanghai Municipal Education Commission (09YZ132), and Shanghai Municipal Health Bureau (2009Y91).

REFERENCES

1. Yan, M. Y.; Chien, S. Y.; Kuo, S. J.; Chen, D. R.; Su, C. C. Tanshinone IIA inhibits BT-20 human breast cancer cell proliferation through increasing caspase 12, GADD153 and phospho-p38 protein expression. *Int. J. Mol. Med.* **2012,** 29, 855-863.
2. Xu, D. F.; Lin, T. H.; Zhang, C. X.; Tsai, Y. C.; Li, S. S.; Zhang, J.; Yin, M.; Yeh, S. Y.; Chang, C. S. The selective inhibitory effect of a synthetic tanshinone derivative on prostate cancer cells. *Prostate* **2012,** 72, 803-816.
3. Li, F. L.; Xu, R.; Zeng, Q. C.; Li, X.; Chen, J.; Wang, Y. F.; Fan, B.; Geng, L.; Li, B. Tanshinone IIA Inhibits Growth of Keratinocytes through Cell Cycle Arrest and Apoptosis: Underlying Treatment Mechanism of Psoriasis. *Evid. Based Complement. Alt. Med.* **2012**.
4. Xie, J.; Wang, H.; Song, T. B.; Wang, Z. R.; Li, F.; Ma, J.; Chen, J.; Nan, Y. Y.; Yi, H.; Wang, W. Tanshinone IIA and astragaloside IV promote the migration of mesenchymal stem cells by up-regulation of CXCR4. *Protoplasma* **2013,** 250, 521-530.
5. Huang, C. Y.; Chiu, T. L.; Kuo, S. J.; Chien, S. Y.; Chen, D. R.; Su, C. C. Tanshinone IIA inhibits the growth of pancreatic cancer BxPC-3 cells by decreasing protein expression of TCTP, MCL-1 and Bcl-xL. *Molecular Medicine Reports* **2013,** 7, 1045-1049.
6. Li, Q.; Wang, Y.; Feng, N. P.; Fan, Z. Z.; Sun, J.; Nan, Y. L. Novel polymeric nanoparticles containing tanshinone IIA for the treatment of hepatoma. *J. Drug Target.* **2008,** 16, 725-732.
7. Xu, S. W.; Liu, P. Q. Tanshinone II-A: new perspectives for old remedies. *Exp. Opin. Therapeu. Patents* **2013,** 23, 149-153.
8. Zhang, W. L.; He, H. L.; Liu, J. P.; Wang, J.; Zhang, S. Y.; Zhang, S. S.; Wu, Z. M. Pharmacokinetics and atherosclerotic lesions targeting effects of tanshinone IIA discoidal and spherical biomimetic high density lipoproteins. *Biomaterials* **2013,** 34, 306-319.

9. Blout, E. R.; Karlson, R. H. Polypeptides. III. The Synthesis of High Molecular Weight Poly-γ-benzyl-L-glutamates1. *J. Am. Chem. Soc.* **1956,** 78, 941-946.
10. Matsumura, Y. Poly (amino acid) micelle nanocarriers in preclinical and clinical studies. *Adv. Drug Deliv. Rev.* **2008,** 60, 899-914.
11. Koo, A. N.; Lee, H. J.; Kim, S. E.; Chang, J. H.; Park, C.; Kim, C.; Park, J. H.; Lee, S. C. Disulfide-cross-linked PEG-poly(amino acid)s copolymer micelles for glutathione-mediated intracellular drug delivery. *Chem. Commun. (Camb)* **2008**, 6570-2.
12. Ding, J. X.; Shi, F. H.; Xiao, C. S.; Lin, L.; Chen, L.; He, C. L.; Zhuang, X. L.; Chen, X. S. One-step preparation of reduction-responsive poly(ethylene glycol)-poly (amino acid)s nanogels as efficient intracellular drug delivery platforms. *Polymer Chem.* **2011,** 2, 2857-2864.
13. Whitehead, K. A.; Langer, R.; Anderson, D. G. Knocking down barriers: advances in siRNA delivery. *Nat. Rev. Drug Dis.* **2009,** 8, 129-138.
14. Fournier, E.; Dufresne, M. H.; Smith, D. C.; Ranger, M.; Leroux, J. C. A novel one-step drug-loading procedure for water-soluble amphiphilic nanocarriers. *Pharm. Res.* **2004,** 21, 962-968.
15. Vauthier, C.; Bouchemal, K. Methods for the Preparation and Manufacture of Polymeric Nanoparticles. *Pharm. Res.* **2009,** 26, 1025-1058.
16. Ma, H.; Fan, Q.; Yu, J.; Xin, J. L.; Zhang, C. Novel Microemulsion of Tanshinone IIA, Isolated from Salvia miltiorrhiza Bunge, Exerts Anticancer Activity Through Inducing Apoptosis in Hepatoma Cells. *Am. J. Chin. Med.* **2013,** 41, 197-210.
17. Chu, T.; Zhang, Q.; Li, H.; Ma, W. C.; Zhang, N.; Jin, H.; Mao, S. J. Development of intravenous lipid emulsion of tanshinone IIA and evaluation of its anti-hepatoma activity in vitro. *Int. J. Pharm.* **2012,** 424, 76-88.
18. Dai, Z. K.; Qin, J. K.; Huang, J. E.; Luo, Y.; Xu, Q.; Zhao, H. L. Tanshinone IIA activates calcium-dependent apoptosis signaling pathway in human hepatoma cells. *J. Nat. Med.* **2012,** 66, 192-201.
19. Yin, P. H.; Wang, Y.; Qiu, Y. Y.; Hou, L. L.; Liu, X.; Qin, J. M.; Duan, Y. R.; Liu, P. F.; Qiu, M.; Li, Q. Bufalin-loaded mPEG-PLGA-PLL-cRGD nanoparticles: preparation, cellular uptake, tissue distribution, and anticancer activity. *Int. J. Nanomed.* **2012,** 7, 3961-3969.

PEG-poly (amino acid)s-encapsulated Tanshinone IIA as potential therapeutics for the treatment of hepatoma

Yan Wang,[1,a] Frankie Costanza,[2,a] Haifan Wu,[2] Daqian Song[1,],Jianfeng Cai[2,]* and Qi Li [1,]*

[1]Department of Medical Oncology, Shuguang Hospital, Shanghai University of Traditional Chinese Medicine,528Zhangheng Road，Shanghai, 201203, China

[2]Department of Chemistry, University of South Florida, 4202 E. Fowler Ave, Tampa, FL 33620

[a] These authors contributed equally to the work.

lzwf@hotmail.com and jianfengcai@usf.edu

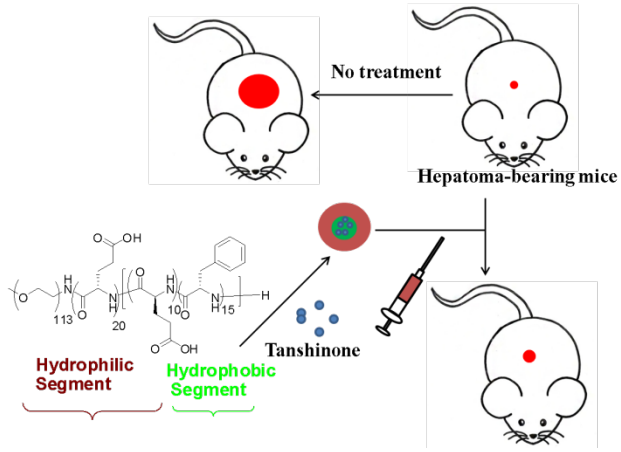

PEG-poly (amino acid)s are used as the novel drug carrier to treat hepatoma.

PEG-poly (amino acid)s are used as the novel drug carrier to treat hepatoma.